



Published in final edited form as:

*J Microelectromech Syst.* 2020 October ; 29(5): 894–899. doi:10.1109/jmems.2020.3000325.

## Microfluidic gasketless interconnects sealed by superhydrophobic surfaces

**Xiaoxiao Zhao,**

Center for BioModular Multiscale Systems for Precision Medicine, Department of Mechanical and Industrial Engineering, Louisiana State University, Baton Rouge, LA 70803, USA

Department of Mechanical Engineering at the University of British Columbia, Okanagan, BC, Canada.

**Daniel S.-W. Park,**

Center for BioModular Multiscale Systems for Precision Medicine, Department of Mechanical and Industrial Engineering, Louisiana State University, Baton Rouge, LA 70803, USA.

**Steven A. Soper,**

Center for BioModular Multiscale Systems for Precision Medicine Departments of Chemistry and Mechanical Engineering, University of Kansas, Lawrence, KS, 66045, USA

**Michael C. Murphy [Member, IEEE]**

Center for BioModular Multiscale Systems for Precision Medicine, Department of Mechanical and Industrial Engineering, Louisiana State University, Baton Rouge, LA 70803, USA

### Abstract

Existing methods for sealing chip-to-chip (or module-to-motherboard) microfluidic interconnects commonly use additional interconnect components (O-rings, gaskets, and tubing), and manual handling expertise for assembly. Novel gasketless superhydrophobic fluidic interconnects (GSFIs) sealed by transparent superhydrophobic surfaces, forming liquid bridges between the fluidic ports for fluidic passages were demonstrated. Two test platforms were designed, fabricated, and evaluated, a multi-port chip system (ten interconnects) and a modules-on-a-motherboard system (four interconnects). System assembly in less than 3 sec was done by embedded magnets and pin-in-V-groove structures. Flow tests with deionized (DI) water, ethanol/water mixture, and plasma confirmed no leakage through the gasketless interconnects up to a maximum flow rate of 100  $\mu\text{L}/\text{min}$  for the multi-port chip system. The modules-on-a-motherboard system showed no leakage of water at a flow rate of 20  $\mu\text{L}/\text{min}$  and a pressure drop of 3.71 psi. Characterization of the leakage pressure as a function of the surface tension of the sample liquid in the multi-port chip system revealed that lower surface tension of the liquid led to lower static water contact angles on the superhydrophobic-coated substrate and lower leakage pressures. The high-density, rapidly assembled, gasketless interconnect technology will open up new avenues for chip-to-chip fluid transport in complex microfluidic modular systems.

## Keywords

Interconnects; Gasketless; Superhydrophobic Surfaces; Embedded Magnets; Passive Alignment Structures

---

## I. Introduction

Lab-on-a-chip technologies are widely applied in the life sciences and potentially in clinical diagnostics such as analyzing DNA or RNA, and capturing circulating tumor cells, exosomes, and bacteria [1–9]. They integrate chemical analytical functions on fluidic chips (or systems), which automate sophisticated sample or liquid manipulations and high-throughput screening. One class of integrated microfluidic systems for lab-on-a-chip technologies are modular microfluidic systems [7–9]. Modular microfluidic systems require assembly of fluidic modules together or onto a fluidic motherboard or stacking modules. Each module can be used as both a stand-alone device and a replaceable unit without rebuilding the entire modular fluidic system.

However, sealing chip-to-chip (or module-to-motherboard) interconnects is complex and limits their availability to non-expert users. Previously, research on microfluidic chip-to-chip interconnects usually utilized complex interconnect components such as O-rings, gaskets, or tubing [7, 10–15]. They commonly require long prototype development, substantial cost, assembly expertise, and the potential for unpredictable dead volumes as a result.

The ability to seal fluidic ports for the chip-to-chip interconnects with predictable low dead volume and no additional interconnect components is important for the utilization of modular microfluidic systems for clinical applications. Ease of assembly by non-expert users without sacrificing performance will be also critical for point-of-care applications. In order to facilitate the possible commercialization of modular microfluidic systems, there is an immediate demand for a simple, low cost, and rapid sealing strategy of the chip-to-chip (or module-to-motherboard) microfluidic interconnects for non-expert end users.

A novel microfluidic gasketless interconnect was developed to transport fluid between two assembled component chips, which were sealed by spin coating superhydrophobic films around the two vertically aligned circular fluidic ports [16]. The gasketless superhydrophobic fluidic interconnect (GSFI) was formed by a liquid bridge spanning the physical gap, that acts as the fluid passage. The gaps were established using passive kinematic constraints [17, 18]. The failure or leakage pressure for the GSFI was calculated using the Young-Laplace equation. Pressures were measured for a total of 99 injection molded COC assemblies and matched the predicted values. The maximum pressure measured was 3 psi for a 3  $\mu\text{m}$  gap. However, there were several limitations for the prototype assemblies. First, the assembled chips had no microchannels, which would increase the pressure drop and thus demand a higher leakage pressure for the GSFIs. Second, only one through-hole interconnect was demonstrated, while many modular microfluidic systems have multiple interconnects between the chips. Third, the opaque superhydrophobic coating on the microfluidic chips was not applicable for optical observation. Fourth, only deionized (DI) water was demonstrated for the GSFIs, while many microfluidic systems use reagents

with lower surface tensions, which requires successful demonstration of the technology with a wide range of liquids with varying surface tensions.

Novel microfluidic gasketless interconnects sealed by transparent, superhydrophobic surfaces for sealing multiple microfluidic interconnects with connecting microchannels were demonstrated. Two microfluidic test platforms were evaluated for assessing the performance of the GSFIs: a multi-port chip system, with ten fluidic interconnects in series, and a modules-on-a-motherboard system, that modelled a typical modular format and had two fluid interconnects between each module and the motherboard. The flow tests with different liquids were carried out to determine whether there was any leakage from the GSFIs for the two test platforms as a function of flow rate. The variation of the leakage pressure in the multi-port chip system was investigated experimentally for sample liquids with a wide range of surface tensions.

## II. Methods

### A. Gasketless superhydrophobic fluid interconnects

The interconnects developed to realize integrated microfluidic systems for lab-on-a-chip technologies in this work are the microfluidic gasketless interconnects sealed by parallel superhydrophobic surfaces (contact angle  $\approx 150^\circ$ ) as shown in Fig. 1. Two nominally, concentric through-holes in two chips (chip A and chip B) or in a module on a motherboard are exactly constrained by passive alignment structures (3 pairs of pin-in-V-groove structures; not shown) to form the gasketless interconnects and to allow the passage of fluids through the interconnects. Passive alignment structures enable simultaneous alignment of multiple interconnects, and they can be manufactured using the established mass production techniques such as injection molding and hot embossing. Passive alignment structures also determine the gap between the two mating surfaces of two chips (or a module and a motherboard) [17, 18].

The leakage pressures for the gasketless interconnects depend on the gap between the mating surfaces, the water contact angle of the liquid on the superhydrophobic surfaces, and the surface tension of the liquid [16]. Given the water contact angle and the surface tension of the liquid, the gap between the mating surface plays a major role on the leakage pressure of the gasketless interconnects, so a nominal gap of  $10\ \mu\text{m}$  was chosen for the two GSFI test platforms.

### B. Test platforms

The first test platform demonstrated for the gasketless superhydrophobic fluid interconnects was a multi-port chip system with ten gasketless interconnects in series. Three-dimensional schematics of the multi-port chip system, with components are shown in Figs. 2(a) and 2(b). Each polymer chip has fluidic microchannels as well as fluidic reservoirs (or ports) on one side and passive alignment structures for assembly on the other side (three pairs of pin-in-V-groove structures with hemispherical tipped posts and V-grooves). Magnet receiving ports were included at the mating surfaces of two chips (four magnet receiving ports on each surface of the chips). Magnet receiving ports were placed away from the functional

microchannels so that the use of magnets does not limit the applications of the gasketless superhydrophobic fluid interconnects.

The second test platform demonstrated for the GSFIs was a modules-on-a-motherboard system with four gasketless interconnects in the form of the mini-universal molecular processing system (uMPS) as shown in Fig. 2(c). The mini-uMPS consists of two task specific modules, one for cell selection and the second for solid phase extraction, and a motherboard. The cell selection module was designed with multiple sinusoidal microchannels [19], fluidic inlet and outlet, three hemispherical tipped posts for alignment, and four magnet receiving ports for assembly. The solid phase extraction module was designed with arrays of cylindrical pillars [20], a fluidic inlet and outlet, three hemispherical tipped posts for alignment, and four magnet receiving ports for assembly. The motherboard was designed with a main fluidic inlet and outlet, three V-grooves for alignment and four magnet receiving ports for assembly for each module (total of eight magnet receiving ports for two modules), and the connecting microchannels.

### C. Test platform fabrication

Brass molds for hot embossing both the multi-port chip and modules-on-a-motherboard platforms were designed using AutoCAD (AutoCAD® 2019, Autodesk, Inc., San Rafael, CA). The AutoCAD designs were converted to instructions for the milling machine using GibbsCAM (3D Systems, Moor-park, CA).

Brass molds were micromilled for each testbed using a micromilling machine (MMP, Kern Mikrotechnik GmbH, Eschenlohe, Germany). For the multi-port chip system, two molds were used for the front, containing fluidic channels, and back sides, with the alignment structures and fluid port, of the substrate. For the modules-on-a-motherboard system two molds were produced for both the two modules and the motherboard.

Poly(methyl methacrylate) (PMMA) was used for both substrates and cover sheets for both testbeds. Substrates were double-sided hot embossed in 3 mm thick PMMA (HEX-02, Jenoptik AG, Jena, Germany). Hot embossing was done at a molding force of 20 kN, a molding temperature of 160°C for 2 minutes, and demolded at a temperature of 90°C.

After cutting the multi-port chip, motherboard, and module substrates, to the required sizes from the hot embossed polymer parts, the fluidic through-holes were mechanically drilled in each multi-port chip, module, and motherboard using a 1/32 drill bit in a drill press (MicroLux, Berkeley Heights, NJ).

All of the molded PMMA components and 250  $\mu\text{m}$  thick cover plates were cleaned using a cleaning protocol [21] and dried in a convection oven at 85°C overnight. Thermal fusion bonding of the cover sheets with the multi-port chips, modules, and motherboards was done by clamping the cover sheets and the multi-port chips, modules, and motherboards between two glass plates, using paper clips to apply the bonding pressure, and putting the whole setup in a convection oven at 105°C for 2 hours.

Coating of the superhydrophobic films needed to be applied on the mating surfaces between the chips or between the modules and the motherboard. Transparent superhydrophobic films

with mixtures of dual-sized silica particles and epoxy resin [22] were spin coated on the two mating surfaces. The silica nano-particle diameters were 200 nm and 55 nm and sized to give a hierarchical structure and to be transparent under the visible spectrum. The spin coating was done at 1,500 rpm for 60 sec. To prevent the coating solution from entering the fluidic ports, the coating solution was evenly spread on the polymer substrates before spin coating.

Prior to assembly of the two bonded multi-port chips, the disc magnets were mounted in the magnet receiving ports by a super glue (Scotch super glue 101, 3M United States, Saint Paul, MN).

#### D. Test platform assembly

Three pairs of pin-in-V-groove structures and four pairs of magnets were utilized during assembly of the two multi-port chip system and the modules-on-a-motherboard system (or the mini-uMPS).

#### E. Flow tests and pressure measurements

A computer-controlled syringe pump (NE-4002X, New Era Pump Systems Inc., Farmingdale, NY) was used to pump fluids into the multi-port chip system and the modules-on-a-motherboard system at flow rates 0 to 100  $\mu\text{L}/\text{min}$ . A commercial microfluidic pressure sensor (MPS, Elveflow, Paris, France) was connected to the test platform to measure the fluid leakage pressure of the gasketless interconnects.

Fluids with different surface tensions were obtained by using mixtures of ethanol and DI water. The method of Vazquez, *et al.* was used to formulate mixtures of ethanol and water with surface tensions ranging from 38.56 mN/m to 72.75 mN/m [23].

### III. Results and Discussion

#### A. Test platform fabrication and assembly

When fluids pass through the interconnects from chip A to chip B (or module to motherboard), the fluids pass through liquid bridges spanning the gaps between the chips. Formation of the liquid bridges are governed by the superhydrophobic surfaces surrounding the fluidic ports. The superhydrophobic surface essentially prevented the lateral leakage of liquid bridges with a potential energy barrier induced by capillary forces as a seal between two vertically aligned fluidic ports. The superhydrophobic fluid interconnects demonstrated in this work are 'gasketless' without the need for any additional components, such as O-rings or gaskets.

Figure 3 shows scanning electron microscope (SEM) images of the edge of a through-hole, and a close-up view of the superhydrophobic film around the through-hole made by the modified spin-coating method. The polymer surfaces around the fluidic ports were covered with nanoparticles, indicating a superhydrophobic surface. In contrast, no coating of the superhydrophobic film was present on the inner wall of the through-hole, so the inner surfaces of the interconnects as shown are not superhydrophobic, and they have the intrinsic material properties of the polymer (water contact angle of  $68^\circ$ ) without surface modification.

Three pairs of the passive alignment structures (pin-in-V-groove structures with hemispherical tipped posts and V-grooves) and four pairs of magnets were utilized during assembly of both the multi-port chip and the modules-on-a-motherboard systems. The passive alignment structures allowed not only exact constraint alignment of the two chips but also the nominal gap of 10  $\mu\text{m}$ . The disk magnets provided enough assembly force between the two multi-port chips as well as the modules with the motherboard. Yuen [12] had previously reported the use of magnets for assembly, but they were centered around the fluid interconnect, which still incorporated a gasket material. Figure 4(a) shows two multi-port chips fabricated in PMMA using hot embossing with micromilled brass molds before assembly. The two chips were assembled for the gasketless fluid interconnects with an assembly time of less than 3 sec (see Figure 4(b)). Figure 4(c) shows two modules and one motherboard fabricated in PMMA using hot embossing with micromilled brass molds. The modules and motherboard were also assembled demonstrating the gasketless fluid interconnects between the motherboard and the modules within 3 sec (see Figure 4(d)).

The gap between the multiport chips or between the modules and the motherboard, and the alignment accuracy of the fluidic ports in the multi-port chip system and the modules-on-a-motherboard system are critical for reliable fluidic passages in modular microfluidic systems. The gaps were measured by SEM and port-to-port misalignment was measured by a confocal microscope, and the results were summarized in Table I. The gap for the multi-port chip system ( $13 \pm 3 \mu\text{m}$ ) and modules-on-a-motherboard system ( $11 \pm 2 \mu\text{m}$ ) agreed well with the nominal gap distance of 10  $\mu\text{m}$ . The port-to-port misalignment was  $53 \pm 17 \mu\text{m}$  for the multi-port chip system and  $45 \pm 13 \mu\text{m}$  for the modules-on-a-motherboard system. The high-density, rapidly assembled, gasketless interconnect technology is applicable for chip-to-chip fluid transport in complex microfluidic assemblies.

## B. Flow tests and pressure measurements with water

When the gasketless fluid interconnects in the multi-port chip system were filled with DI water mixed with methylene blue, liquids flowed between the two microfluidic chips, passing sequentially through up to ten gasketless interconnects (see Figure 5). The close-up view of the microfluidic gasketless fluid interconnects confirmed no leakage at the gap between the two multi-port chips (see Figure 6). Without the superhydrophobic films, the interconnects in an identical multi-port chip system leaked immediately at the first interconnect (see Figure 7). The multi-port chip system allowed all fluids (DI water, ethanol/water mixture, or plasma) to successfully pass through all ten fluid interconnects without leakage up to a maximum flow rate of 100  $\mu\text{l}/\text{min}$ .

The performance of the gasketless superhydrophobic fluid interconnects in the mini-uMPS was evaluated with DI water mixed with methylene blue. The superhydrophobic, gasketless interconnects did not leak for fluid flow between the motherboard and two modules for the cell capture and solid phase extraction in the mini-uMPS at flow rate of 20  $\mu\text{l}/\text{min}$  and a pressure drop of 3.71 psi (see Figure 8).

### C. Flow tests and pressure measurements with different surface tension liquids

Many microfluidic systems with fluidic interconnects use reagents with lower surface tensions. In order to demonstrate working gasketless interconnects at a wide range of surface tensions, liquids with surface tension of 72.75 mN/m, 56.41 mN/m, 48.14 mN/m, 42.72 mN/m, and 38.56 mN/m were obtained by adding 0%, 5%, 10%, 15%, and 20% of ethanol in DI water, respectively. The variations of leakage pressure of the multi-port chip system were measured with respect to the surface tension of the sample liquid (see Figure 9). Three pairs of chips were tested for each liquid at each surface tension. As the surface tension of the liquid decreases, the static water contact angle on the superhydrophobic coated substrate also decreases, which leads to lower leakage pressures for the gasketless interconnects. A smaller gap between the chips or between a module and a motherboard, can be utilized for higher leakage pressure of the gasketless interconnects when low surface tension sample liquid is used [16].

## IV. CONCLUSIONS

Rapid sealing for modular microfluidic systems was demonstrated with microfluidic gasketless interconnects. The interconnects were gasketless with liquid bridges formed between the two fluidic ports and sealed by capillary forces generated by superhydrophobic surfaces. The novel superhydrophobic surfaces on polymers were transparent and mechanically robust against manual contact during the assembly process, especially for non-expert users.

In order to demonstrate gasketless superhydrophobic fluid interconnects (GSFIs) for lab-on-a-chip applications, two test platforms were designed, fabricated, and tested: a multi-port chip system with ten interconnects and a modules-on-a-motherboard system (or a mini-uMPS) with four interconnects in series. The use of the embedded magnets and passive alignment structures (pin-in-V-groove structures) enabled rapid alignment and assembly (less than 3 sec). Three pairs of pin-in-V-groove structures with hemispherical tipped posts and V-grooves allowed for the gap distance of 10  $\mu\text{m}$  between the chips (or between the modules and the motherboard). The flow tests in the multi-port chip system with different liquids confirmed no leakage through the ten gasketless superhydrophobic fluid interconnects up to a flow rate of 100  $\mu\text{L}/\text{min}$ . The mini-uMPS demonstrated no leakage of DI water at the flow rate of 20  $\mu\text{L}/\text{min}$  and a pressure drop of 3.71 psi. The variations of leakage pressure were investigated with respect to the surface tension of the sample liquid in the multi-port chip system, and it was found that the lower surface tension of the liquid resulted in a lower static water contact angle on the superhydrophobic substrate and a lower leakage pressure for the gasketless interconnects.

The gasketless superhydrophobic fluid interconnects will be applicable to higher density interconnects for integration of multiple modules on mixed scale motherboards with simple and rapid assemblies.

## Acknowledgment

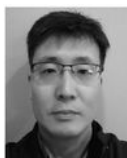
We thank Mr. J. Guy at the Center for Biomodular Multi-Scale Systems (CBMM) at Louisiana State University (LSU) for micromilling of brass mold inserts, and the Center for Advanced Microstructures and Devices (CAMD) at LSU for microfabrication support.

This work was supported by Biotechnology Resource Center (NIH P41EB020594) through the National Institute of Biomedical Imaging and Bioengineering (NIBIB) of the National Institutes of Health (NIH).

## Biographies



**Xiaoxiao Zhao** received his B.S. degree in Mechanical Engineering from University of Shanghai for Science and Technology, PR. China (2014), and his Ph.D. in Mechanical Engineering from Louisiana State University, USA (2019). He is currently a post-doctoral researcher at University of British Columbia, Canada, working on developing non-fluorinated omniphobic papers. His work is focused on developing microfluidic devices and systems, liquid-repellent coatings, ice-repellent coatings, and non-fluorinated strategies for surface treatment.



**Daniel S.-W. Park** received his B.S. degree in Physics from Sung Kyun Kwan University, Seoul, Korea, in 1990, his M.S. degree in Electrical Engineering from Louisiana State University in 1999, and his Ph. D. degree in Electrical Engineering from the University of Texas at Dallas in 2004. He is currently a research associate at the Mechanical and Industrial Engineering and the Center for BioModular Multi-scale Systems (CBMM) in Louisiana State University, working on BioMEMS devices/systems for biomedical applications. His research interests include micro/nano fabrication techniques and their applications to BioMEMS, RF MEMS, and nano-scale devices/systems.



**Steven A. Soper** received his Ph.D. from the University of Kansas in 1989 in Bioanalytical Chemistry. He then did a post-doctoral fellowship at Los Alamos National Laboratory, where he worked on single-molecule detection approaches for DNA sequencing. He is currently a Foundation Distinguished Professor in Biomedical Engineering and Chemistry at



The University of Kansas and Director of the NIH-sponsored Center of BioModular Multiscale Systems for Precision Medicine. His work is focused on developing polymer-based BioMEMS and BioNEMS for cellular and molecular processing for *in vitro* diagnostics; single-molecule DNA/RNA sequencing technologies; and surface modification of polymer micro- and nanochannels. He is also the founder and currently Chief Scientific Officer at BioFluidica, Inc., which is developing microfluidic platforms for the isolation of liquid biopsy markers.



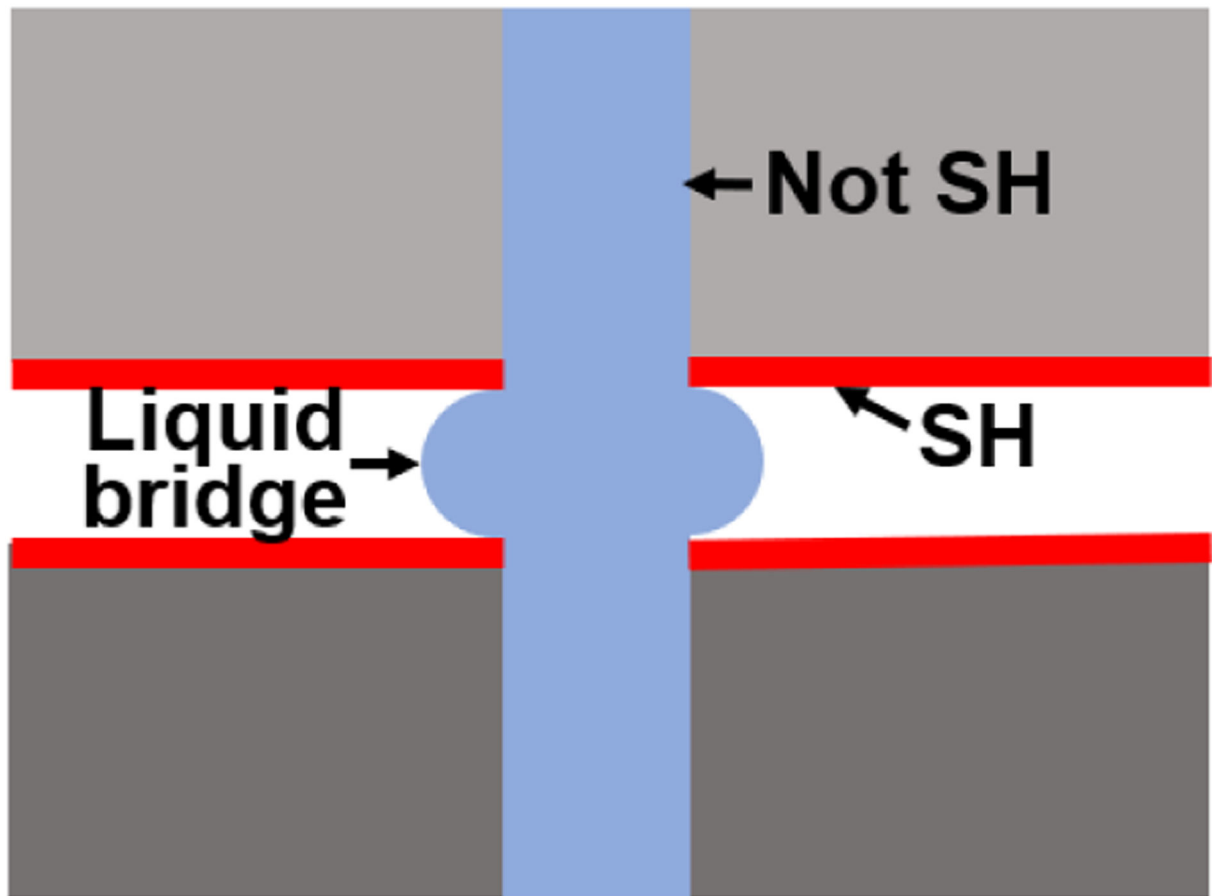
**Michael C. Murphy** received his B.S. degree in Mechanical Engineering (1977) from Cornell University in Ithaca, NY, and an M.S. (1978) in Aeronautics from the California Institute of Technology in Pasadena, CA. He was a member of the technical staff and a staff doctoral fellow at the Hughes Aircraft Company Missile Systems Group (Canoga Park, CA) from 1978–1985. His doctoral and post-doctoral work was at the Massachusetts Institute of Technology (Cambridge, MA) with his Ph.D. (1990) in Mechanical Engineering and research in knee kinematics and control. He was the Roy O Martin Lumber Company Professor in the College of Engineering at LSU and is now an Emeritus Professor of Mechanical Engineering, with research interests in Microfabrication, Bio-MEMS/NEMS, Medical Device Design, and Biomechanics.

## REFERENCES

- [1]. Sin ML, Gao J, Liao JC, and Wong PK, “System Integration - A Major Step toward Lab on a Chip,” *Journal of biological engineering*, vol. 5, pp. 6–6, 2011. [PubMed: 21612614]
- [2]. Xu B, Du W-Q, Li J-W, Hu Y-L, Yang L, Zhang C-C, Li G-Q, Lao Z-X, Ni J-C, Chu J-R, Wu D, Liu S-L, and Sugioka K, “High efficiency integration of three-dimensional functional microdevices inside a microfluidic chip by using femtosecond laser multifoci parallel microfabrication,” *Scientific Reports*, vol. 6, pp. 19989, 01/28/online, 2016. [PubMed: 26818119]
- [3]. Martinez-Cisneros C, da Rocha Z, Seabra A, Valdés F, and Alonso-Chamarro J, “Highly integrated autonomous lab-on-a-chip device for online and in situ determination of environmental chemical parameters,” *Lab on a Chip*, vol. 18, no. 13, pp. 1884–1890, 2018. [PubMed: 29869662]
- [4]. Zhang JM, Ji Q, Liu Y, Huang J, and Duan H, “An integrated micro-millifluidic processing system,” *Lab on a Chip*, vol. 18, no. 22, pp. 3393–3404, 2018. [PubMed: 30280159]
- [5]. Adamski MG, Li Y, Wagner E, Seales-Bailey C, Bennett N, Yu H, Murphy M, Soper SA, and Baird AE, “CD15+ granulocyte and CD8+ T lymphocyte based gene expression clusters for ischemic stroke detection,” *Medical Research Archives; Vol 5 No 11 (2017): Vol.5 Issue 11 - November 2017*, 2017.
- [6]. Jackson JM, Witek MA, Kamande JW, and Soper SA, “Materials and microfluidics: enabling the efficient isolation and analysis of circulating tumour cells,” *Chemical Society Reviews*, vol. 46, no. 14, pp. 4245–4280, 2017. [PubMed: 28632258]
- [7]. Wang H, Chen H-W, Hupert ML, Chen P-C, Datta P, Pittman TL, Goettert J, Murphy MC, Williams D, Barany F, and Soper SA, “Fully Integrated Thermoplastic Genosensor for the Highly Sensitive Detection and Identification of Multi-Drug-Resistant Tuberculosis,” *Angewandte Chemie International Edition*, vol. 51, no. 18, pp. 4349–4353, 2012. [PubMed: 22431490]

- [8]. Kamande JW, Hupert ML, Witek MA, Wang H, Torphy RJ, Dharmasiri U, Njoroge SK, Jackson JM, Aufforth RD, Snaveley A, Yeh JJ, and Soper SA, "Modular Microsystem for the Isolation, Enumeration, and Phenotyping of Circulating Tumor Cells in Patients with Pancreatic Cancer," *Analytical Chemistry*, vol. 85, no. 19, pp. 9092–9100, 2013/10/01, 2013. [PubMed: 23947293]
- [9]. Lee TY, Han K, Barrett DO, Park S, Soper SA, and Murphy MC, "Accurate, predictable, repeatable micro-assembly technology for polymer, microfluidic modules," *Sensors and Actuators B : Chemical*, vol. 254, pp. 1249–1258, 2018/1/01/, 2018.
- [10]. Temiz Y, Lovchik RD, Kaigala GV, and Delamarche E, "Lab-on-a-chip devices: How to close and plug the lab?," *Microelectronic Engineering*, vol. 132, pp. 156–175, 2015/1/25/, 2015.
- [11]. Chen A, and Pan T, "Fit-to-Flow (F2F) interconnects: Universal reversible adhesive-free microfluidic adaptors for lab-on-a-chip systems," *Lab on a Chip*, vol. 11, no. 4, pp. 727–732, 2011. [PubMed: 21109877]
- [12]. Yuen PK, "A reconfigurable stick-n-play modular microfluidic system using magnetic interconnects," *Lab on a Chip*, vol. 16, no. 19, pp. 3700–3707, 2016. [PubMed: 27722698]
- [13]. Gong H, Woolley AT, and Nordin GP, "3D printed high density, reversible, chip-to-chip microfluidic interconnects," *Lab on a Chip*, vol. 18, no. 4, pp. 639–647, 2018. [PubMed: 29355276]
- [14]. Scott A, Au AK, Vinckenbosch E, and Folch A, "A microfluidic D-subminiature connector," *Lab on a Chip*, vol. 13, no. 11, pp. 2036–2039, 2013. [PubMed: 23584282]
- [15]. Chen Y-W, Wang H, Hupert M, Witek M, Dharmasiri U, Pingle MR, Barany F, and Soper SA, "Modular microfluidic system fabricated in thermoplastics for the strain-specific detection of bacterial pathogens," *Lab Chip*, vol. 12, pp. 3348–3355, 2012. [PubMed: 22859220]
- [16]. Brown CR, Zhao X, Chen PC, Park T, You BH, Park DS, Soper SA, Baird A, and Murphy MC, "Leakage pressures for gasketless superhydrophobic fluid interconnects (GSFI) for modular lab-on-a-chip systems," *Nature Micro-system & Nanoengineering*, Under Review.
- [17]. You BH, Chen P-C, Park DS, Park S, Nikitopoulos DE, Soper SA, and Murphy MC, "Passive micro-assembly of modular, hot embossed, polymer microfluidic devices using exact constraint design," *J Micromech Microeng*, vol. 19, pp. 125025, 2009.
- [18]. You BH, Park DS, Rani SD, and Murphy MC, "Assembly of Polymer Microfluidic Components and Modules: Validating Models of Passive Alignment Accuracy," *Journal of Microelectromechanical Systems*, vol. 24, no. 3, pp. 634–650, 2015. [PubMed: 31814689]
- [19]. Adams AA, Okagbare PI, Feng J, Hupert ML, Patterson D, Göttert J, McCarley RL, Nikitopoulos D, Murphy MC, and Soper SA, "Highly Efficient Circulating Tumor Cell Isolation from Whole Blood and Label-Free Enumeration Using Polymer-Based Microfluidics with an Integrated Conductivity Sensor," *Journal of the American Chemical Society*, vol. 130, no. 27, pp. 8633–8641, 2008/7/01, 2008. [PubMed: 18557614]
- [20]. Campos CDM, Gamage SST, Jackson JM, Witek MA, Park DS, Murphy MC, Godwin AK, and Soper SA, "Microfluidic-based solid phase extraction of cell free DNA," *Lab on a Chip*, vol. 18, no. 22, pp. 3459–3470, 2018. [PubMed: 30339164]
- [21]. Park DSW, Hupert ML, Witek MA, You BH, Datta P, Guy J, Lee JB, Soper SA, Nikitopoulos DE, and Murphy MC, "A titer plate-based polymer microfluidic platform for high throughput nucleic acid purification," *Biomedical Microdevices*, vol. 10, no. 1, pp. 21–33, 2008/2/01, 2008. [PubMed: 17659445]
- [22]. Zhao X, Park DS, Choi J, Park S, Soper SA, and Murphy MC, "Robust, transparent, superhydrophobic coatings using novel hydrophobic/hydrophilic dual-sized silica particles," *Journal of Colloid and Interface Science*, vol. 574, pp. 347–354, 2020/8/15/, 2020. [PubMed: 32335484]
- [23]. Vazquez G, Alvarez E, and Navaza JM, "Surface Tension of Alcohol Water + Water from 20 to 50 .degree.C," *Journal of Chemical & Engineering Data*, vol. 40, no. 3, pp. 611–614, 1995/5/01, 1995.

# Chip A (or Module)



# Chip B (or Motherboard)

**Fig. 1.** Schematic showing liquid flow from one microfluidic chip to the other; the lateral expansion of the liquid bridge was prevented by capillary forces induced by the superhydrophobic (SH) coating.

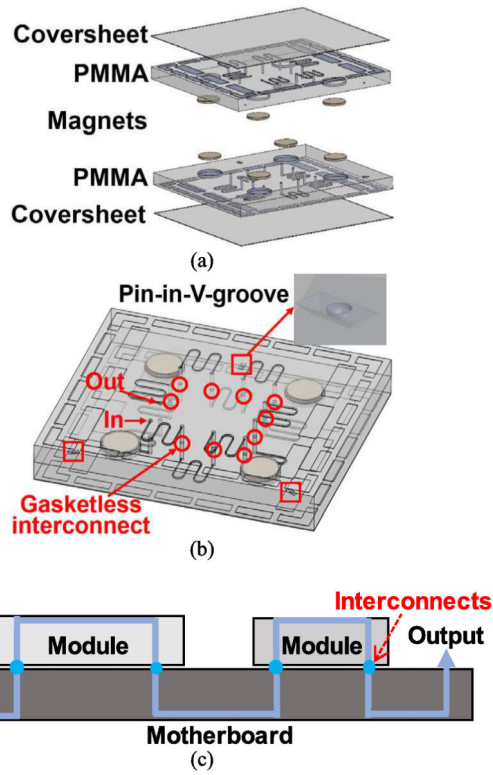


**Fig. 2.** 3-D schematics of the multi-port chip system including coversheets and substrates in PMMA and magnets (a) before and (b) after assembly; The right top in Fig. 2(b) shows one of the three pin-in-V-groove alignment structures shown in red squares. Ten interconnects are shown in red circles. (c) 2-D schematic of the modules-on-a-motherboard system with four gasketless superhydrophobic fluid interconnects.

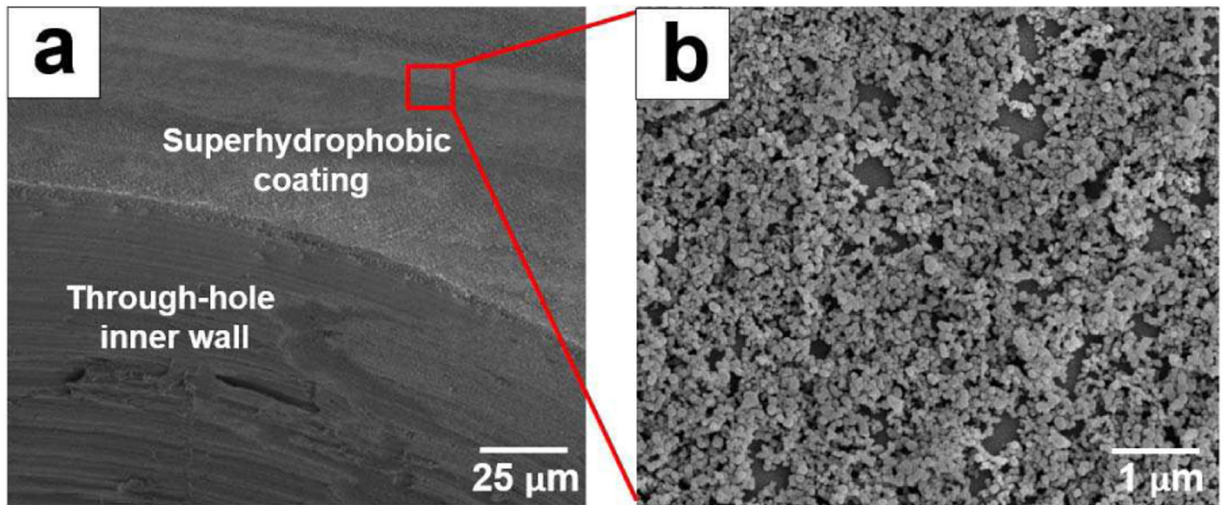


**Fig. 3.** SEM images of (a) the edge of a through-hole, and (b) a close-up view of the superhydrophobic coating surface with mixtures of silica particles and epoxy resin.

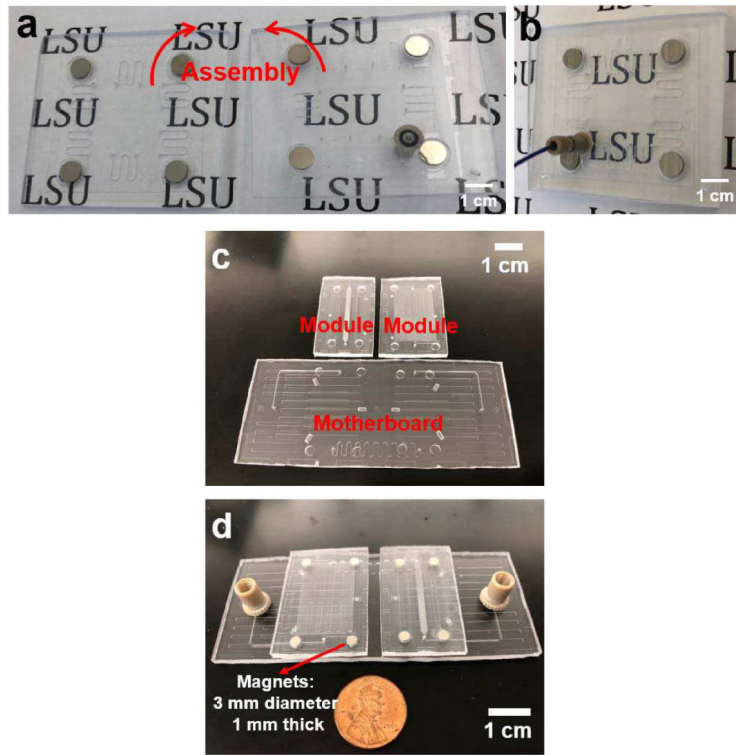


**Fig. 4.** The multi-port chip system fabricated in PMMA by double-sided hot embossing with two brass molds (a) before and (b) after assembly, and (c) Two modules and one motherboard in PMMA fabricated by double-sided hot embossing with two brass molds for the mini-uMPS; (d) The modules and motherboard after assembly by passive alignment structures and magnets.

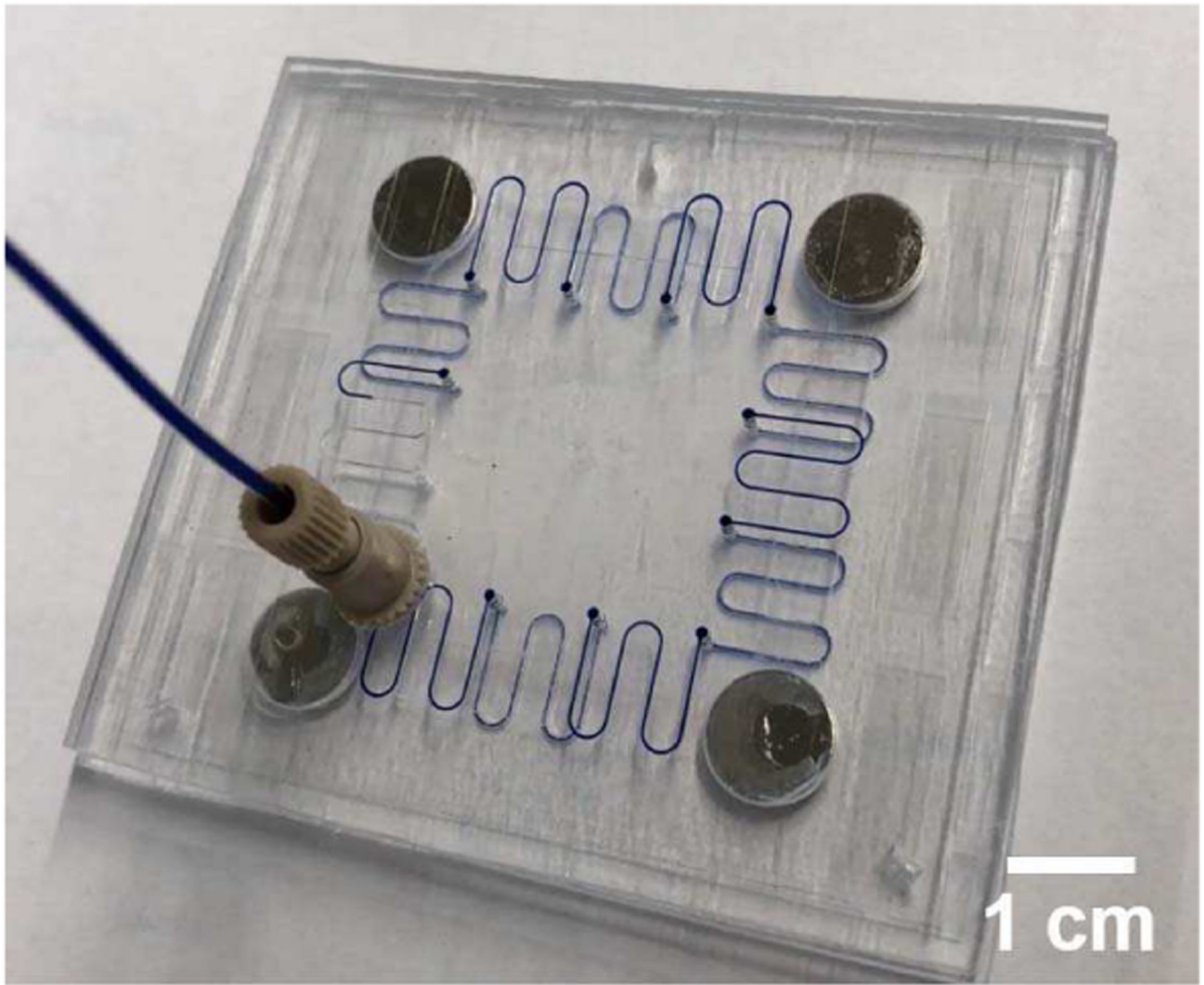


**Fig. 5.** DI water flow through ten gasketless superhydrophobic fluid interconnects in the multi-port chip system; Methylene blue was added to DI water to aid visual clarity.

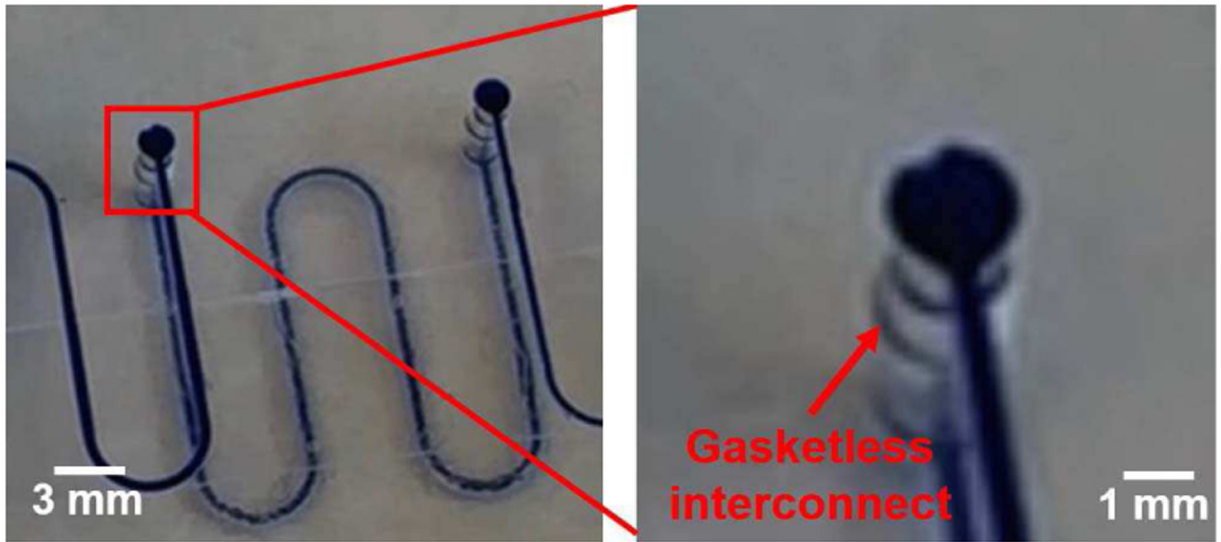


**Fig. 6.** Microfluidic superhydrophobic fluid interconnects with microchannels in the upper and lower chips (left) and a close-up view of a gasketless interconnect (right), which show no leakage at the gap between two chips of the multi-port chip system.



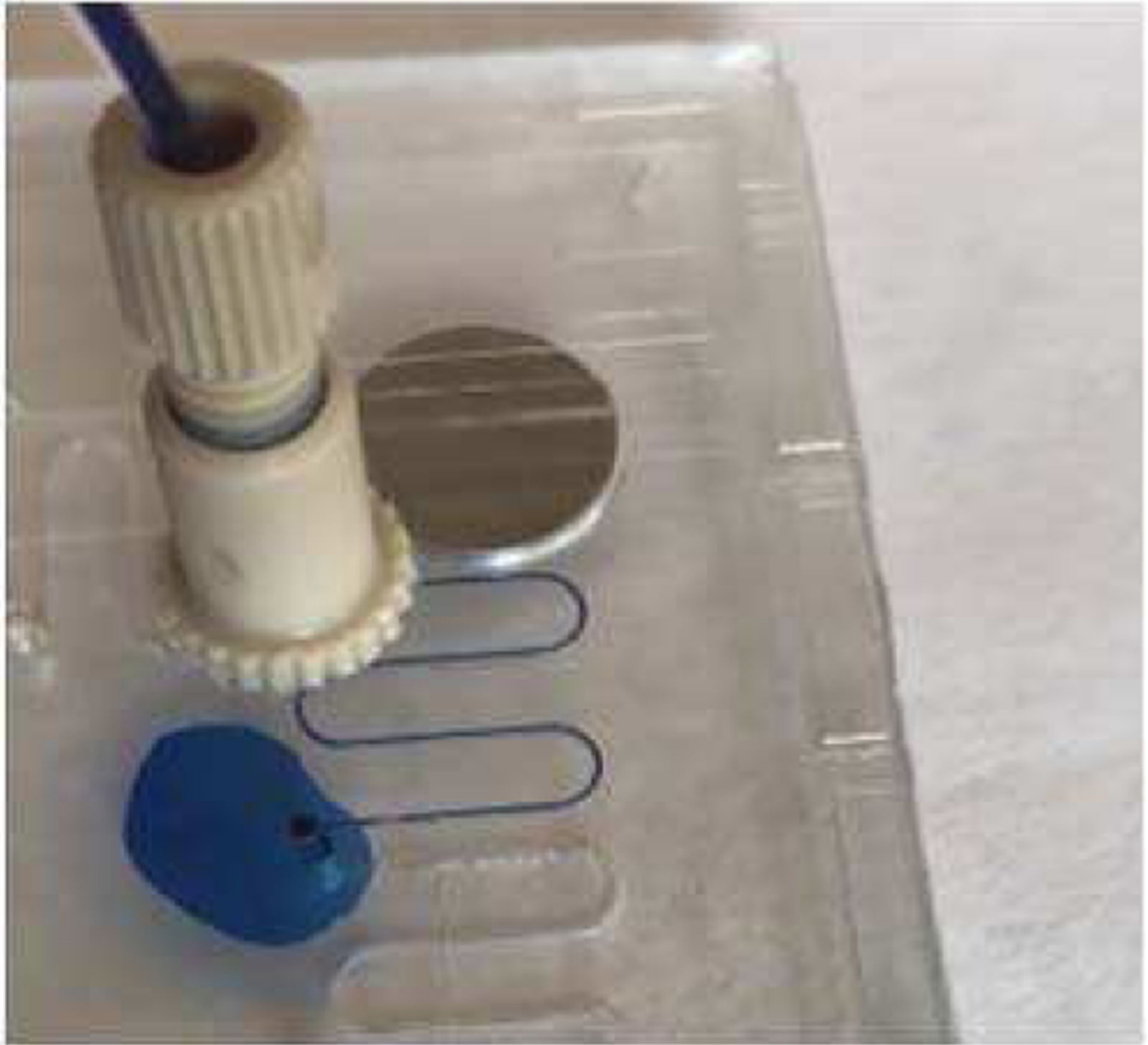


**Fig. 7.** Fluidic leakage observed for the gasketless interconnects without being sealed by superhydrophobic surface.

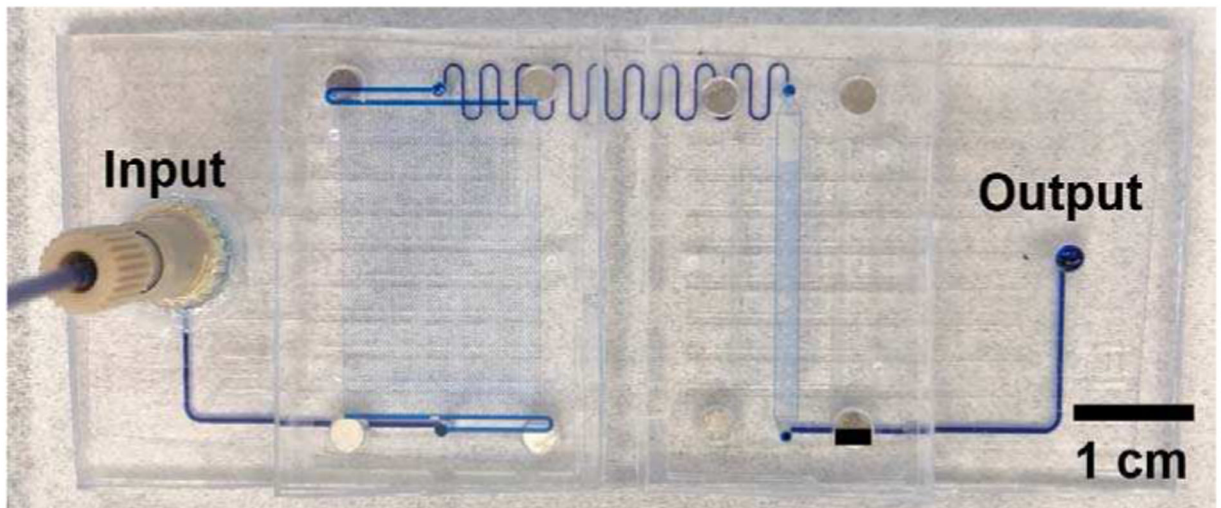


**Fig. 8.** DI water flow through the cell capture module and the solid phase extraction module on the motherboard in the mini-uMPS at  $20 \mu\text{l}/\text{min}$  showing no leakage at the four gasketless superhydrophobic fluid interconnects.

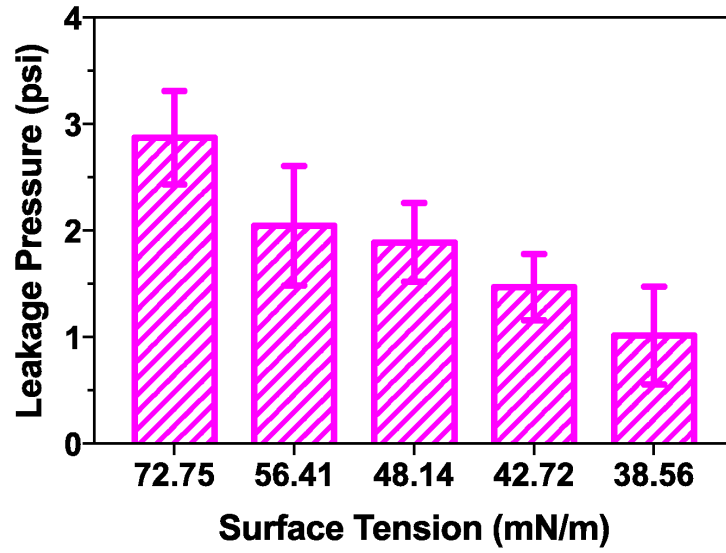


**Fig. 9.** The variation of leakage pressure of the multi-port chip system as a function of the surface tension of the sample liquid. The liquids of surface tension of 72.75 mN/m, 56.41 mN/m, 48.14 mN/m, 42.72 mN/m, and 38.56 mN/m were obtained by adding 0%, 5%, 10%, 15%, and 20% of ethanol in DI water, respectively.

**Table I**

Chip-to-chip gap distance, and port-to-port misalignment on the multi-port chip system and the module-on-amotherboard system (mini-uMPS)

	Gap ( $\mu\text{m}$ )	Misalignment ( $\mu\text{m}$ )
Multi-port chip system	$13 \pm 3$	$53 \pm 17$
Mini-uMPS	$11 \pm 2$	$45 \pm 13$

Author Manuscript

Author Manuscript

Author Manuscript

Author Manuscript